

Crash Analysis And Design of Multi-Cell Octagonal S-Shape Members Under Axial And Oblique Impacts

Sobhan Esmaeili-Marzdashti¹, Tamer A. Sebaey^{2,*}, Sadjad Pirmohammad¹,
Sareh Esmaeili-Marzdashti³

¹(Department Of Mechanical Engineering, Faculty Of Engineering, University Of Mohaghegh Ardabili, Ardabil,179, Iran.)

²(Mechanical and Industrial Engineering Department, College Of Engineering, Qatar University, 2713, Doha, Qatar.)

³ (Department Of Mechanical Engineering, Polytechnique Montreal, P.O. Box 6079, Station Downtown Montreal, Quebec, Canada.)

* Corresponding author email:sebaey@qu.edu.qa

Abstract : Crashworthiness of the structures used in automotive is widely being addressed as it is defining the safety. The present article aims to investigate crushing performance under axial and oblique impact performed under 10°, 20° and 30° for different cross-section configurations of S-shaped longitudinal members. Modeling and numerical analysis are carried out using finite element code LS-DYNA. The model was validated using experimental data. The complex proportional assessment (COPRAS) method is used to provide optimized alternative design by considering two conflicting criteria, energy absorption (EA) and peak crushing force (PCF). The results indicate that the structures (at which four blades connect the outer and the inner walls) with inner reinforcing blades have a high crash performance than the others (without connecting blades). Besides, the blades in multi-cell members, which connect the middle of edges (T4), lead to superior response in comparison with the other ones (which connect corners). Finally, dimensions (the wall thickness and the distance of inner and outer tubes) of T4 are optimized by design of experiment and response surface methodology techniques.

Keywords: Crashworthiness, Design of experiment, Impact, Multi-cell, Optimization

I. INTRODUCTION

To increase safety level in transportation systems for preventing loss of life and injuries in accidents, there is a need for components that can absorb impact energy and prevent harm and damage in critical parts. Energy absorbers are utilized to reduce the undesirable effects of accidents and dissipate the kinetic energy of impact via plastic deformation. As an energy absorber in crashworthiness applications such as trains, cars, ships, aircrafts and other high-volume industrial products, the thin walled structures have been widely used to ensure crash safety due to their lightweight, low cost and high energy absorption [1,2]. The members encountered the impact are expected to absorb maximum energy and possess minimum mass. So, due to having the high specific strength and more energy absorption than the other materials, the use of aluminum has become more and more predominant [3]. The early investigations in energy absorbers are focusing on steel columns for their low costs and high ductility [4]. For better understanding the crashing behavior in aluminum columns, comprehensive studies have been conducted using the numerical and experimental methods. In this regard, Alexander [5] first presented an analytical solution for circular tubes to obtain mean crushing force under axial impact. Then, the models were used by Wierzbicki and Abramowicz [6] to predict the crushing response of aluminum tubes under dynamic and static loading. Abramowicz and Jones [7,8] and Langseth and Hopperstad [9] validated experimentally the theoretical predictions. By comparing the results with the numerical simulations, Kim and Wierzbicki [10] acquired the analytical solution for the crushing resistance of thin-walled S-shaped frames with rectangular cross-sections. Khalkhai et al. [11] expressed a combined analytical and experimental research of thin-walled S-shaped square tubes subjected to the quasi-static axial crushing. Optimization problem, about energy absorption of the S-rail, has been solved by Han and Yamazaki [12].

Over the past few years there has been a growing interest in the use of multi-cell members as energy absorption applications. Fang et al. [13] studied the crashing behavior of foam-filled bitubal circular tubes subjected to axial loading to optimize them in crashworthiness. Chen and Wierzbicki [14] found that the multi-cell members absorb greater specific energy than the conventional simple tubes. Ohkami et al. [15] and Hidekazu Nishigaki et al. [16] studied the collapse behavior of S-shaped beams. They performed dynamic and static collapsing tests. Zhang and Saigal [17] have also investigated the effects of different cross-section reinforcement strategies during impacts. They concluded that applying the reinforcement in structures increases the total energy absorption. Various arrangements of blades on the s-shaped tubes were studied by Hosseini-Tehrani and Nikahd [18,19]. They focused on a remarkable arrangement of straight and sideling blades.

Oblique loading can interpret all the situations in crashing events for pieces designed for axial loading. The energy absorber system needs to endure an impact angle larger than 30° [20]. In order to carry out a complete simulation, oblique loading should be taken into account. Tran et al. [21] implemented the analytical modeling of dynamic oblique loading conditions, which were validated by the numerical results, by considering an oblique impacting boundary conditions and exploring related effects. Elmarakbi et al. [22] carried out numerical studies on energy absorption characteristics of simple and multi-walled S-shaped longitudinal members with four kinds of cross-sections under axial quasi static loading. The multi-cell members are the tubes with blades which connect the inner tubes with the outer ones. Their results reveal that the multi-walled members with octagonal cross-sections for two types of materials, mild steel and aluminum are introduced as optimized shapes which better react in crash procedure.

The current paper aims to investigate the specific energy absorption (SEA) and peak crushing force (PCF) for multi-cell S-shaped longitudinal members by applying two kinds of blades to connect inner tubes and outer ones in octagonal cross-sections. Then COPRAS method is used to choose the best configuration with the high crashworthiness performance by considering two conflicting criteria, (SEA) and (PCF). In order to know the behavior of changing geometric parameters in crushing problems and optimized their performance, response surface models (RSM) and design of experiment (DOE) techniques are also considered.

II. SPECIMEN GEOMETRY AND MOLDING

The aim of this paper is to investigate the crushing behavior of different S-shape multi-wall structures with octagonal cross sections and various types of blades for both axial and oblique impacts. The proposed specimen configurations are shown in Fig. 1. Three different types of tubes are proposed; single-cell one single-cell (Fig. 1a), two doubly-cells (Fig. 1b and 1e) and four multi-cell forms (Fig. 1c, d, f and g). Different cross-sectional configurations with various layouts of the blades are considered for the comparative study. The description of each configuration is summarized as:

T1: single tube;

T2: bitubal tube I;

T3: corner blades which connect the corners of the outer and inner walls,

T4: middle blades which link the middle of the edges of inner and outer tubes,

T5: bitubal tube II;

T6: blades directly coupling the middle of the outer walls with the inner wall corners.

T7: blades connecting the outer corners with the middle of inner walls.

The difference between bitubal type I and II is that the inner tube rotates 22.5° relative to the outer one in type II. The mentioned sections possess the same perimeter of 534mm for outer tubes and the total length of $L=1000$ mm [22]. It is remarkable that, in order to maintain the same mass, different values are set to wall thickness. The dimensional model is shown in Fig. 2.

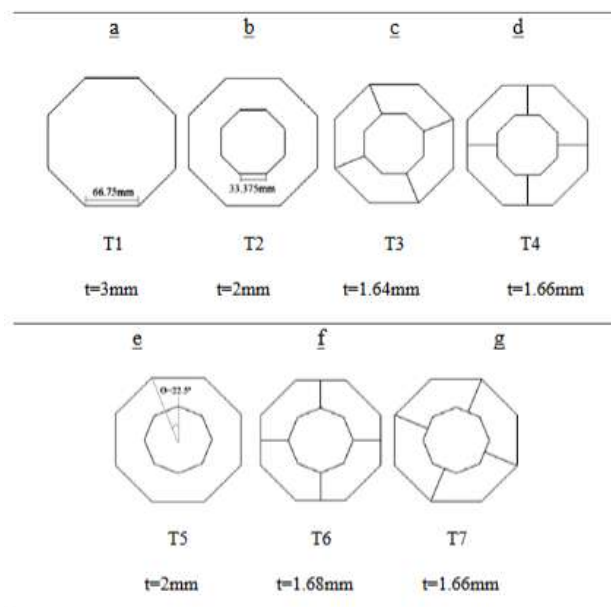


Figure 1: Sectional configurations of multi-cell S-shape tubes with the same mass but different wall thicknesses.

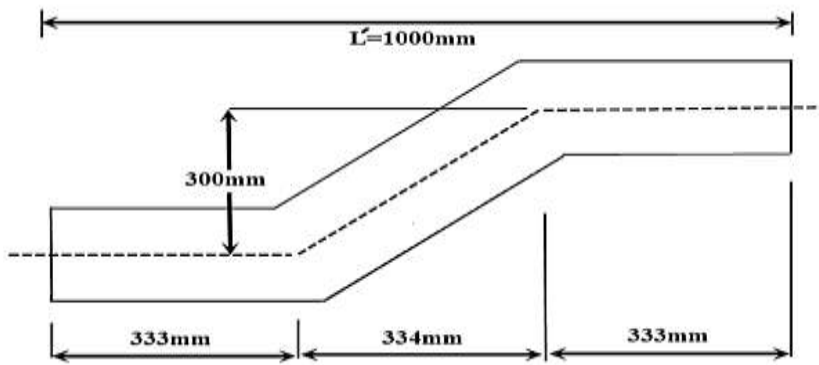


Figure 2: Dimensions of an S-shaped longitudinal member

Non-linear finite element code, LS-DYNA [23], is employed to analyze collapse mode and energy absorption of thin-walled components with different sections under compression load. Specimens are modeled using the quadrilateral full-integration (ELFORM 2) shell element with four nodes and with five integration points through the thickness. In order to achieve an acceptable finite element model, several mesh convergence analyses are accomplished.

The axial and oblique loads applied on the s-shaped tubes are modeled by the rigid wall planar moving force available in LS-DYNA. In order to simulate the dynamic crushing condition, a 600 kg lumped mass with an initial velocity of $V=15$ m/s strikes the end of the S-rail as shown in Fig. 3. The rear end of the S-shape tube has fully clamped and in contrast, the front end, just in the direction of impact, is considered without any constraint. The contact between the bodies during collapse is modeled as node to surface contact algorithm. For both static and dynamic friction, a friction coefficient of 0.15 is adopted for all contacting surfaces [24]. The S-shaped tubes material are considered as aluminum alloy AA6060. The material characteristics is measured using tensile test as shown in Fig. 4. The values of the engineering constants are: Poisson's ratio $\nu=0.3$, yield strength $S_y=80$ MPa, ultimate strength $S_U=173$ MPa, density $\rho=2700$ kg/m³, and Young's modulus $E=68.2$ GPa.

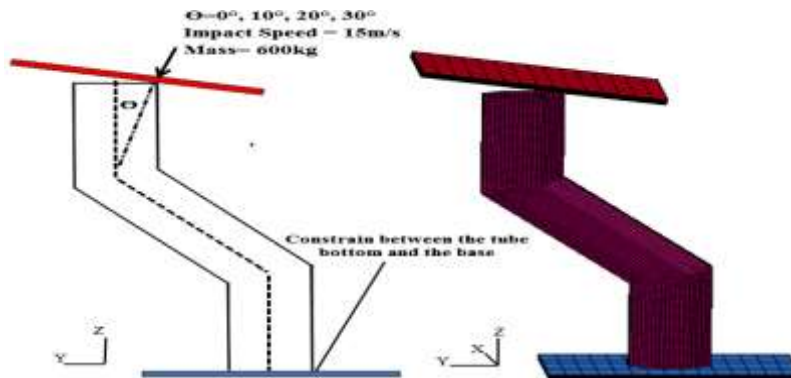


Figure 3: Boundary and loading conditions assumed in the finite element modeling

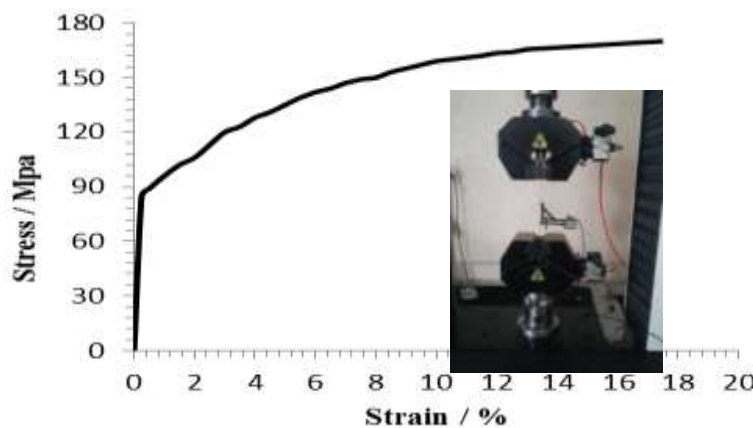


Figure 4: Stress-strain curve of aluminum AA6060

Before running the FE models, it is required to validate them by comparing their results with experimental ones. For this purpose, experiments are carried out on circular tubes using the drop hammer test machine. Experimental dynamic tests are performed on circular tubes of 60 mm diameter, 150 mm length and 2.1 mm wall thickness. The drop-weight test performed using hammers mass of 110 kg and impact velocity of 13 m/s. The experimentally obtained load–displacement responses are compared with the numerical predictions. Hammer mass crushed the circular tubes 90 mm. Fig. 5 compares the crushing force versus displacement and the final deformation patterns between FE simulation and experimental tests of circle tubes. It can be noted that the FE simulation is in good agreement with the experiment in terms of force–displacement curve and final deformed profile of circle tube (Fig. 5). Therefore, the FE modeling established in this paper is considered sufficiently accurate for further comparative analyses.

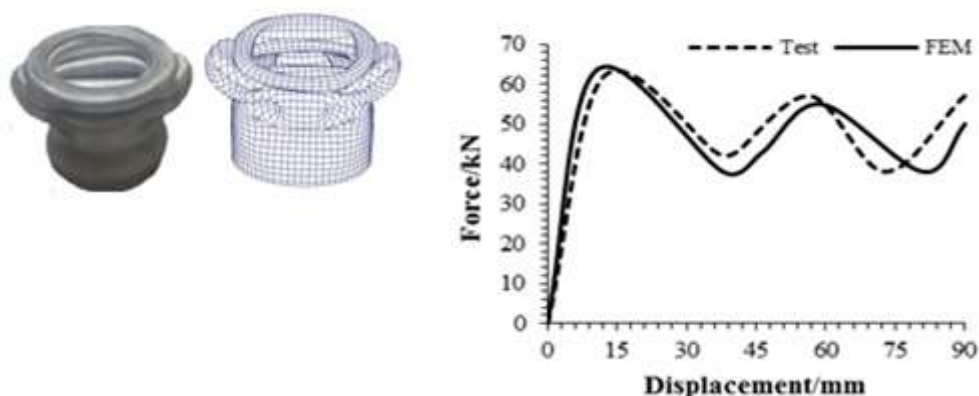


Figure 5: Numerical and experimental results for the circular tubes

III. CRASHWORTHINESS ASSESSMENT

Structural crashworthiness indicator under oblique loading

In crashworthiness problems, the energy absorption capacity of multi-cell S-shaped longitudinal members is computed by specific energy absorption (SEA), which is acquired by dividing energy absorption capability (EA) by the total mass of structures. Therefore, by increasing the EA and decreasing weight of members, the SEA as beneficial indicator goes up. Energy absorption (EA) and specific energy absorption (SEA) are determined as:

$$EA = \int_0^{\delta} F(x) dx \tag{1}$$

$$SEA = \frac{EA}{m} \tag{2}$$

where EA is the absorbed energy, δ is the effective stroke length, F(x) presents the instantaneous crushing force in the axial and oblique direction, and m is the total mass of the member. High specific (SEA) capability and a low peak crushing force (PCF) should be adopted to prevent severe damage and injury during a collapse.

For such a multi criteria decision making (MCDM) process, the complex proportional assessment (COPRAS) is used as the ranking method [25,26]. This method introduces the best decision by considering both the ideal and the ideal-worst solutions of alternative designs under the presence of mutually conflicting criteria [27-31]. The procedure is described in certain details as follows:

- a) Select the available set of the most important criteria which depicts the alternatives.
- b) Generate the initial decision- matrix, X.

$$X = [X_{ij}]_{mn} = \begin{bmatrix} x_{11} & x_{12} & \dots & x_{1n} \\ x_{21} & x_{22} & \dots & x_{2n} \\ \dots & \dots & \dots & \dots \\ x_{m1} & x_{m2} & \dots & x_{mn} \end{bmatrix} \tag{3}$$

where X_{ij} is the performance value of i^{th} alternative design with respect to j^{th} criterion, m is the number of comparative alternative design and n is the number of criteria.

- c) Normalize the decision matrix (r_{ij}) in order to obtain the dimensionless values of different criteria and compare them as:

$$R = [r_{ij}]_{mn} = \frac{X_{ij}}{\sum_{i=1}^m X_{ij}} \quad (4)$$

- d) Identify the weight of each criterion (W_j) by using individual weightage method [32,33]. The indicators considered herein are the specific energy absorption (SEA) and the peak crushing force (PCF). SEA is assumed more significant than PCF. So, the weight for SEA is assigned as 0.1875 and for PCF is 0.0625 by considering four angle strokes.

- e) Determine the weighted normalized decision matrix, D

$$D = [y_{ij}]_{mn} = r_{ij} \times W_j \quad (5)$$

Where r_{ij} is the normalized performance value of i^{th} criterion with respect to j^{th} alternative and W_j is the weight of i^{th} criterion. The sum of dimensionless weighted normalized values of each criterion is always equal to the weight for that criterion:

$$\sum_{i=1}^n y_{ij} = W_j \quad (6)$$

- f) Sums of the weighted normalized values are computed for both the beneficial attributes and non-beneficial attributes. Due to considering more weight to the SEA as an ideal criterion in comparison with PCF as a non-ideal criterion, the value of Eq. 9 becomes greater than Eq.10.

$$S_{+i} = \sum_{j=1}^n y_{+ij} \quad (7)$$

$$S_{-i} = \sum_{j=1}^n y_{-ij} \quad (8)$$

where y_{+ij} and y_{-ij} are the weighted normalized values of the beneficial and non-beneficial criteria, respectively. The better alternative design is obtained by the greater value of S_{+i} and the lower value of S_{-i} . Also, the sums of S_{+i} and S_{-i} of the alternatives are always respectively equal to the sums of weights for the beneficial and non-beneficial criteria as expressed by:

$$S_{+} = \sum_{i=1}^m S_{+i} = \sum_{i=1}^m \sum_{j=1}^n y_{+ij} \quad (9)$$

$$S_{-} = \sum_{i=1}^m S_{-i} = \sum_{i=1}^m \sum_{j=1}^n y_{-ij} \quad (10)$$

- g) Determine the relative significance or priorities for each candidate alternative (Q_i).

$$Q_i = S_{+i} + \frac{S_{-\min} \sum_{i=1}^n S_{-i}}{S_{-i} \sum_{i=1}^n (S_{\min} / S_{-i})} \quad (i = 1, 2, \dots, n) \quad (11)$$

where $S_{-\min}$ is the minimum value of S_{-i}

- h) Determine the quantitative utility in a complete ranking of the alternatives (U).

$$U_i = \frac{Q_i}{\sum_{i=1}^7 Q_i} \times 100\% \tag{12}$$

where Q_{\max} defines the maximum relative significance which is the best option for the alternative selection decision.

IV. NUMERICAL RESULTS AND DISCUSSIONS

In this study, the influences of the load angle and importance of the geometric parameters on the S-shaped tubes responses (SST) under four stroke angle impact loading (0° , 10° , 20° , 30°) are investigated. Numerical analyses are carried out to compare the crush behavior of the seven types of SST (S-shaped tubes). It can be noted that the deflection is specifically defined as the vertical displacement, δ , of the rigid wall with respect to various load angle and initial velocity of 15 m/s. The effective stroke length is taken as 0.4 L, while L is the total length of the energy absorbing structure. The dynamic force-displacement curves of the proposed SST subjected to the four crushing angles are plotted separately in Fig. 6 and Fig. 7. Each rising and falling in load-deflection curves obviously implies the existence of a folding in the structures. By increasing load angle θ from 0° to 30° , the arrival time to the peak increases. Although they are small, differences between the crashworthiness responses can be seen on the plots.

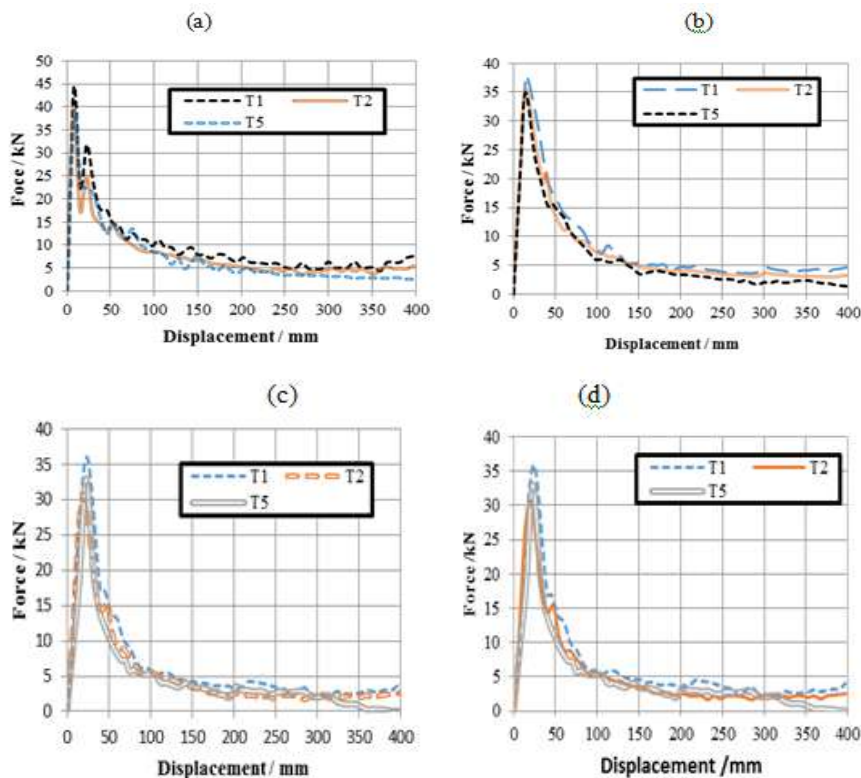


Figure 6: Crushing force vs. displacement curve for specimens without blades; (a) $\theta = 0^\circ$, (b) $\theta = 10^\circ$, (c) $\theta = 20^\circ$ and (d) $\theta = 30^\circ$

Due to the presence of the inside end parts offset (D), less energy is absorbed by the tubes which leads the deformation mode to change from axial progressive folding dominant to global bending one. In this case, the impact force reaches the highest value and then drops sharply. The observed load-deflection characteristics of the SST can be further understood by looking at the final stage deformation modes of some of the tubes at typical load angles, Fig. 8.

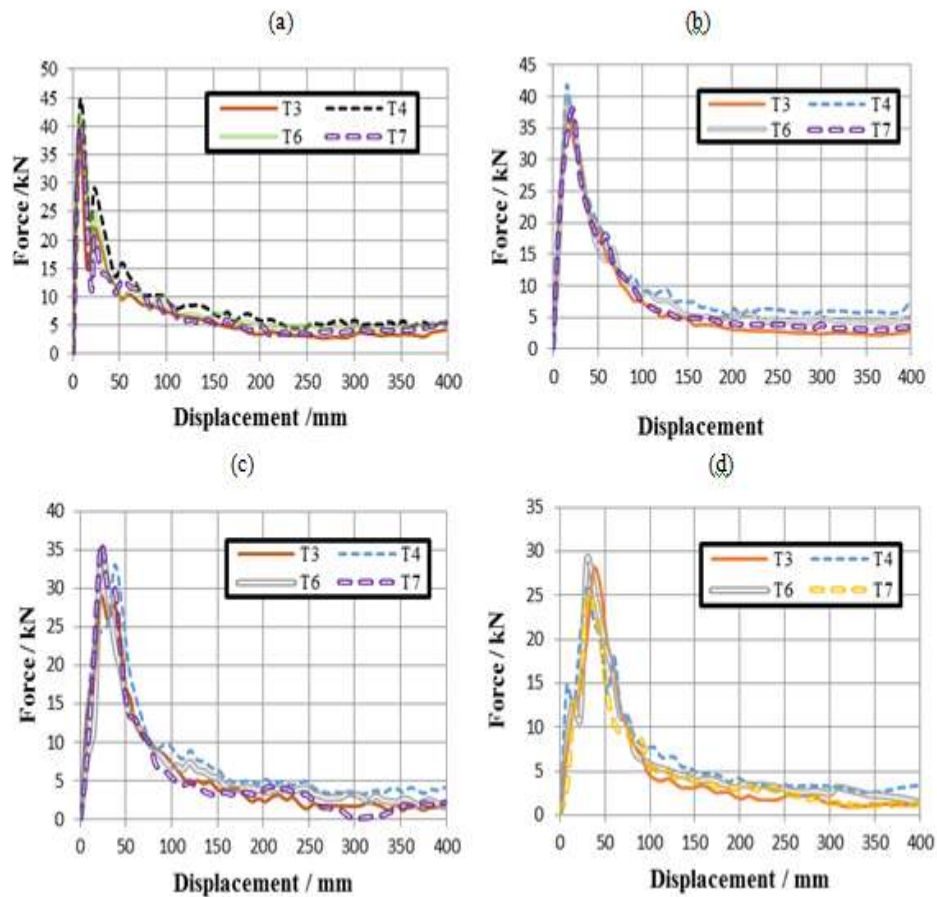


Figure 7: Crushing force vs. displacement curve for specimens with blades; (a) $\theta = 0^\circ$, (b) $\theta = 10^\circ$, (c) $\theta = 20^\circ$ and (d) $\theta = 30^\circ$

Fig 9a and 9b show the crashworthiness indicators (EA and PCF) calculated from the numerical results, for all the members with same mass and under multiple load studied. As it is evident in Figs. 9b, by increasing loading angle from $\theta=0^\circ$ to $\theta=30^\circ$, the PCF decreases. It is noteworthy that bitubal S-shaped tubes with blades connecting the middle sides of inner and outer tubes (T4) has more PCF than bitubal structures with blades connecting the corners of inner and outer ones (T3). Besides, according to the rotational effect of inner tube respect to the outer one on PCF value, multi-cell S-shaped tubes introduced by T7 achieve less PCF than multi-cell S-shaped ones named T6. It is clear in Fig. 9b that the higher PCF value belongs to S-shaped tube T4 in stroke angle of $\theta=0^\circ$ and 10° and T1 and T6 in crushing angle of $\theta=20^\circ$ and 30° . In general, multi-cell forms of SST absorb more energy than single and double-cell structures with the same mass and under multiple load conditions. Similar result was noticed by Wu et al. [34]. The authors of that paper concluded that the higher the number of cells, the more efficient energy absorption characteristics. The comparison between various structures shows that the amount of this criterion in bitubal structures with interaction between middle sides by using blades (T4) is more than the interaction between the corner sides of inner and outer tubes by utilizing blades (T3). On the other hand, rotating inner tubes with respect to the outer ones in bitubal structures has an undesirable effect on absorbing energy. Consequently, T7 absorb less energy than T6 under axial and oblique dynamic loading. It can be expressed that the number of corners and the types of blades play a significant role for energy absorbers in crash problems. Fig. 9 illustrates that, for all loading angle, the highest energy absorbing indicators belong to T4 configuration.

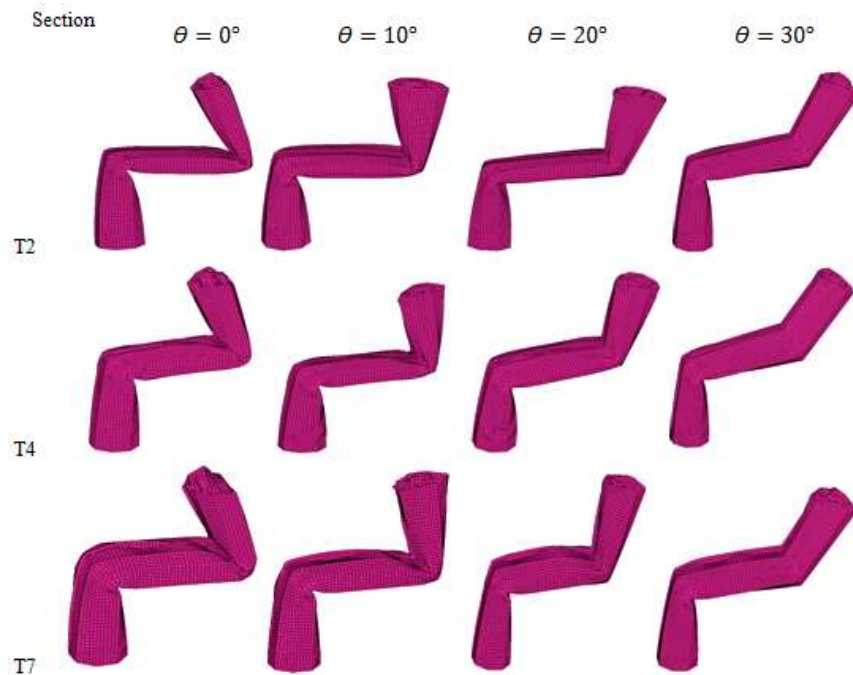
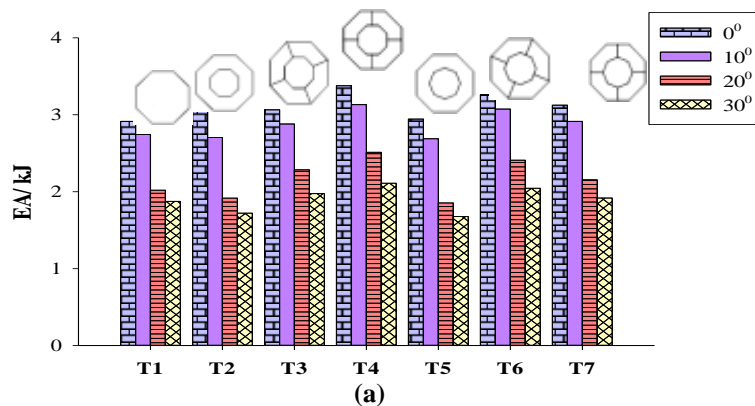


Figure 8: Deformation modes of multi-cell tubes under different loading angles

The COPRAS method is applied on the LS-DYNA results of multi-cell members investigated in this paper to rank them in terms of crashworthiness capability. The COPRAS aims to choose the best energy absorber in terms of the high crash performance. In order to diminish the damage received to any structure which is in direct relationship with high amount of EA as a beneficial attribute and low amount of PCF as a non-beneficial attribute, COPRAS calculation is reassumed for those mentioned criteria (totally 8 indicator) in four crushing angles. Due to assuming EA as a major indicator than PCF in this essay, the weights of 0.1875 is assigned to EA as and 0.0625 is given to PCF in four angle stroke. According to COPRAS steps, the decision-matrix, weighted normalized decision matrix is generated in Table 1, 2. According to Table 3, the final ranking of s-shaped tubes (i.e. T1-T7) is obtained as 5-6-3-1-7-2-4. This means that the best choice of these seven alternative sections with same mass and under multiple loads is T4.

Consequently, by increasing the number of corners (N) in S-shaped tubes and also by a rotating the inner tubes by 22.50°, with respect to the outer tube, structural crashworthiness performs better. The number of corners for T1 through T7 is 8, 16, 16, 16, 24, 20, and 20, respectively. Among mentioned tubes, T4, which possesses 24 corners and parallel tubes, has the best crashworthiness capability. Therefore, by utilizing COPRAS method, the rank of 100% is assigned to it. Moreover, by comparing the performance of Type 2 and Type 5 with the same corners, it is deduced that Type 2 with parallel tubes has higher crashworthiness than the other. In addition, the comparison of the results between T1, T2, and T5 shows that the crushing performance of bitubal structures without blades are less than simple tubes. Consequently, it can be expressed that blade plays a significant role in crushing performance.



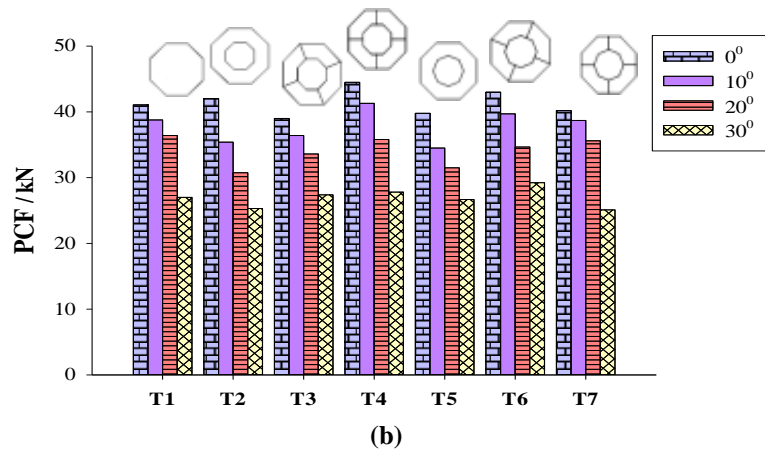


Figure 9. Performance comparisons under different loading angles: (a) EA, (b) PCF.

Table 1. Decision matrix.

Angle	$\theta = 0^\circ$		$\theta = 10^\circ$		$\theta = 20^\circ$		$\theta = 30^\circ$	
	EA	PCF	EA	PCF	EA	PCF	EA	PCF
T1	2.915	40.06	2.745	38.78	2.205	36.41	1.875	28.05
T2	3.085	41.49	2.705	35.39	1.917	30.75	1.72	25.3
T3	3.065	39.12	2.88	36.4	2.285	33.59	1.975	27.38
T4	3.378	44.51	3.132	41.31	2.513	35.09	2.112	27.81
T5	2.945	39.78	2.688	34.48	1.853	31.49	1.676	26.7
T6	3.26	42.5	3.075	39.72	2.41	34.67	2.045	29.24
T7	3.125	40.19	2.915	38.7	2.153	35.6	1.918	25.12

Table 2. Normalized decision matrix.

Angle	$\theta = 0^\circ$		$\theta = 10^\circ$		$\theta = 20^\circ$		$\theta = 30^\circ$	
	EA	PCF	EA	PCF	EA	PCF	EA	PCF
T1	0.1338	0.1392	0.1362	0.1464	0.1437	0.1531	0.1407	0.1477
T2	0.1416	0.1442	0.1343	0.1336	0.1250	0.1294	0.1291	0.1334
T3	0.1407	0.1359	0.1429	0.1374	0.1489	0.1414	0.1482	0.1445
T4	0.1551	0.1546	0.1555	0.1559	0.1638	0.1477	0.1581	0.1466
T5	0.1352	0.1383	0.1334	0.1302	0.1208	0.1325	0.1258	0.1408
T6	0.1497	0.1477	0.1526	0.1499	0.1571	0.1459	0.1535	0.1542
T7	0.1435	0.1397	0.1447	0.1461	0.1403	0.1498	0.1440	0.1324

Table 3. Results of COPRAS method

Section	T1	T2	T3	T4	T5	T6	T7
S_+	0.10401	0.0994	0.10892	0.11861	0.0966	0.11491	0.10737
S_-	0.03666	0.0338	0.03496	0.03781	0.0338	0.03736	0.03550
Q_i	0.13874	0.1370	0.14536	0.15234	0.1342	0.14903	0.14323
U_i	91.0970	89.999	95.4488	100	88.126	97.8541	94.0454
Rank	5	6	3	1	7	2	4

V. RESPONSE SURFACE MODELS

According to Section 4, the bitubal structure with four connecting blades in octagonal tubes named Type 4 is introduced as the best alternative sections by considering COPRAS method. In this section, response surface methodology (RSM) in terms of design of experiments (DOE) is used to know the behavior of changing geometric parameters in crushing problems and optimized their performance [35, 36]. Fig. 10 displays the flowchart of implementing response surface methodology for optimization problem.

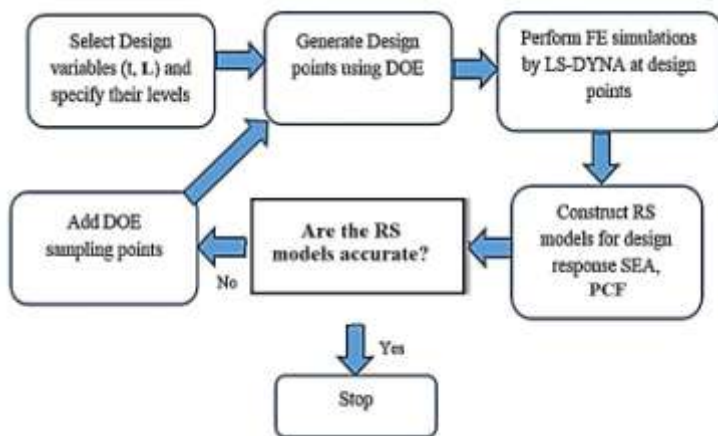
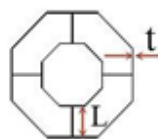


Figure 10: Flow chart showing the steps of creating the RS models.

In the first step of optimization, the design points are determined by the design of experiment (DOE) techniques such as CCD (central composite design) in the design-expert software. The wall thickness (t) and the length of the blades (L) are selected to be the independent variables. The ranges and step size of the two design variables are summarized in Table 4. Based on the optimal tube size in previous section, the dimensions are chosen in such a way to cover the typical range of tube sizes generally used in crashworthiness applications, such as in automotive body [37]. Table 5 shows the design matrix predictions. Structures with dimensions of the design points are then analyzed in LS-DYNA to find the crush indicators (SEA1-4 and PCF1-4) under multiple loading angles (0°, 10°, 20°, and 30°).

Table 4 Range and step size of design variables and impact angle of Type 4 S-shaped tubes.

Parameters	Lower bound	Upper bound	Step size
Wall-thickness <i>t</i> (mm)	1.5	2.5	0.5
The blade length <i>L</i> (mm)	35	55	10
Load angle θ (°)	0	30	10



Geometry

Table 5. The design matrix

Iteration	t (mm)	L(mm)	SEA ₁	PCF ₁	SEA ₂	PCF ₂	SEA ₃	PCF ₃	SEA ₄	PCF ₄
1	2.5	35	0.672	75.65	0.58	60.86	0.484	54.97	0.415	48.41
2	2.5	45	0.847	79.36	0.78	66.87	0.681	60.56	0.634	53.56
3	2	45	0.696	60.92	0.66	52.13	0.628	46.41	0.622	41.78
4	2	55	0.881	69.83	0.82	59.67	0.731	54.09	0.674	45.68
5	2	45	0.696	60.92	0.66	52.13	0.628	46.41	0.622	41.78
6	1.5	55	0.815	52.38	0.81	46.21	0.671	38.39	0.638	33.42
7	1.5	45	0.662	48.42	0.58	44.62	0.542	34.52	0.508	27.82
8	2	45	0.696	60.92	0.66	52.13	0.628	46.41	0.622	40.78
9	2	35	0.624	56.78	0.58	49.13	0.571	43.35	0.548	39.45
10	2	45	0.696	60.92	0.66	52.13	0.628	46.41	0.622	41.78
11	2	45	0.696	60.92	0.66	52.13	0.628	46.41	0.622	41.78
12	1.5	35	0.521	38.52	0.43	37.05	0.395	26.12	0.381	20.75
13	2.5	55	1.031	90.48	0.95	84.51	0.881	54.36	0.733	66.42

Fig. 11 and Fig. 12 show the 3-D diagrams of SEA and PCF at different geometrical and loading conditions. They illustrate the influence of geometrical changes on crashworthiness performance in various impact angles. For all impact loading conditions, by increasing t and L the amount of SEA1-4 and PCF1-4 increased. Conclusion, enlarging t and L have a negative effect on PCF and in contrast a positive effect on SEA in the current study for the s-shaped members of Type 4.

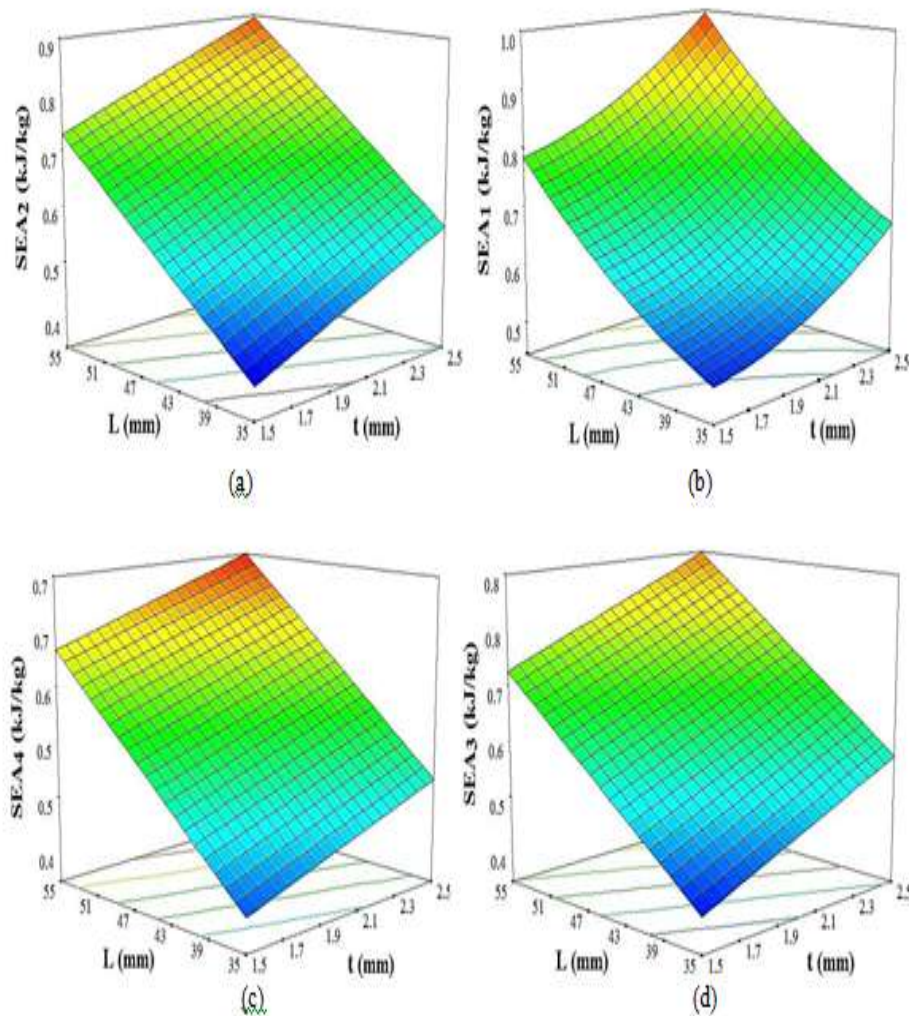


Figure 11: Variation of SEA₁₋₄ with L & t for the impact angles; (a) $\theta = 0^\circ$, (b) $\theta = 10^\circ$, (c) $\theta = 20^\circ$, and (d) $\theta = 30^\circ$

RSM is employed to predict the crashworthiness indices of SEA and PCF of the T4 tubes under axial and oblique impact loading (0° , 10° , 20° , and 30°). These indices are then to be maximized or minimized for optimization. The desirability objective function vs design variables L and t is shown in Figs. 13. It is evident in these figures that the optimal points meet the same geometrical parameters properties, which are as follows: $L=55$ mm, and $t=1.5$ mm. In general, increasing the thickness of the tube and increasing the blade length show the way to optimum design with the limits of the current study introduced in Table 4.

VI. CONCLUSIONS

In this paper the crashworthiness characteristics of single, doubly and multi-cell S-shaped tubes with octagonal cross-section (totally seven structures) and with the presence of five blades to connect inner and outer tubes in bitubal structures have been investigated. The loading angles ranges from 0° to 30° . Moreover, non-linear finite element code LS-DYNA is employed to establish the model. The model is validated by experimental results for the simple extrusion circular tubes under axial dynamic loading.

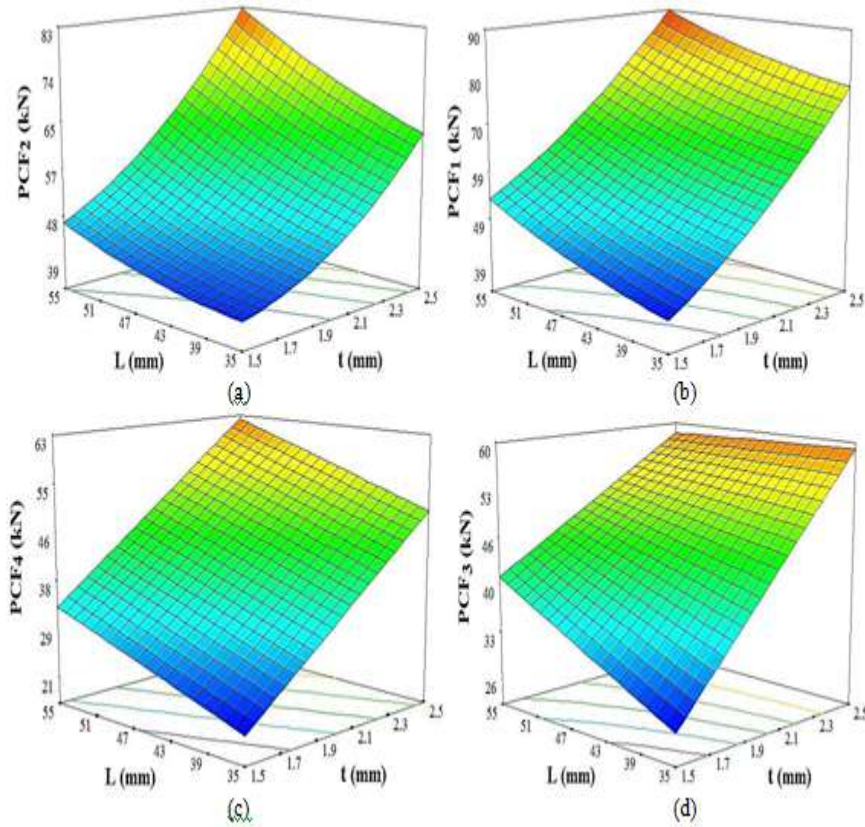


Figure 12: Variation of PCF_{1-4} with L & t for the impact angles; (a) $\theta = 0^\circ$, (b) $\theta = 10^\circ$, (c) $\theta = 20^\circ$, and (d) $\theta = 30^\circ$

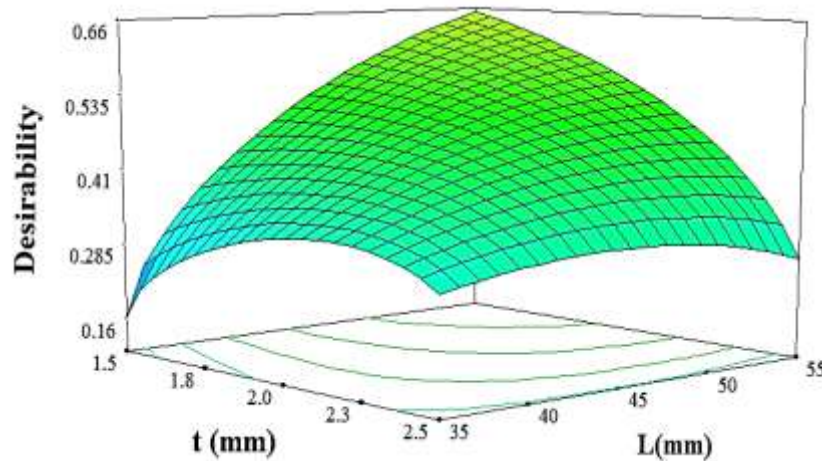


Figure 13: Ideal surface of desirability for the design variables

Due to presence of internal end parts offset, all the s-shape tubes deform as global bending multiple impact angle, leading to the decrease in SEA and PCF as two conflicting criteria in this paper. The complex proportional assessment method (COPRAS) is chosen for the multi-criteria decision making process (MCDM) by considering beneficial and non-beneficial criteria. It is extracted that the bitubal S-shaped tubes with mid-edge blades connector (namely T4) has got high crashworthiness. On the other hand, the number of corners (N) in section shape and the rotation of inner tube in bitubal members play a significant role to improve the crushing performance. Within the scope of the present study, more corners are counted in bitubal members with the blades connecting mid-edge leads to absorb more energy than members with the blades connecting corner-edge. Design of experiment (DOE) method and response surface methodology (RSM) are considered for all impact angles to describe the effects of geometrical parameters changes on the T4. The results shows that increasing the

tube blade length and decreasing the tube wall-thickness resulted in the optimum design, as per the desirability objective function.

REFERENCES

- [1]. Happian-Smith J. An introduction to modern vehicle design, (Oxford: Reed Educational and Professional Publishing Ltd.; 2002)
- [2]. L. Ying, X. Zhao, M. Dai, S. Zhang, and P. Hu, Crashworthiness design of quenched boron steel thin-walled structures with functionally graded strength, *International Journal of Impact Engineering*, 95, 2016,72-88.
- [3]. H.S. Kim, New extruded multi-cell aluminum profile for maximum crash energy absorption and weight efficiency, *Thin-walled Structures*, 40, 2002,311–27.
- [4]. M. Seitzberger, F.G. Rammerstorfer, R. Gradinger, H.P. Degischer, M. Blaimschein, and C. Walch, Experimental studies on the quasi-static axial crushing of steel columns filled with aluminum foam, *International Journal of Solids Structures*, 37, 2000, 4125–47.
- [5]. JM Alexander, An approximate analysis of the collapse of thin cylindrical shells under axial loading, *The Quarterly Journal of Mechanics and Applied Mathematics*, 13, 1960,10–5.
- [6]. T. Wierzbicki and W Abramowicz, On the crushing mechanics of thin-walled structures, *Journal of Applied Mechanics*, 50, 1983,727–34.
- [7]. W. Abramowicz and N Jones, Dynamic axial crushing of square tubes, *International Journal of Impact Engineering* 2,1984, 179–208.
- [8]. W. Abramowicz and N Jones, Dynamic progressive buckling of circular and square tubes, *International Journal of Impact Engineering* 4, 1986, 243–70.
- [9]. M. Langseth and O.S. Hopperstad, Static and dynamic axial crushing of square thin-walled aluminum extrusions, *International Journal of Impact Engineering*, 18, 1996, 949–68.
- [10]. H.S. Kim and T. Wierzbicki, Closed-form solution for crushing response of three-dimensional thin-walled “S” frames with rectangular cross-section, *International Journal of Impact Engineering* 30, 2004, 87–112.
- [11]. A. Khalkhali, A. Darvizeh, A. Masoumi, M. Jafari, and A. Shiri, Experimental and numerical investigation into the quasi-static crushing behavior of the S-shape square tubes, *Journal of Mechanics*, 27, 2011, 585–596.
- [12]. J. Han and K. Yamazaki, Crashworthiness optimization of S-shape square tubes, *International Journal of Vehicle Design*, 31, 2003, 72–85.
- [13]. J. Fang, Y. Gao, G. Sun, Y. Zhang, and Q. Li, Crashworthiness design of foam-filled bitubal structures with uncertainty, *International Journal of Non-Linear Mechanics*, 67, 2014, 120–132.
- [14]. W. Chen and T. Wierzbicki, Relative merits of single-cell, multi-cell and foam-filled thin-walled structures in energy absorption, *Thin-Walled Structures* 39, 2001, 287–306.
- [15]. Y. Ohakami, K. Takada, K. Motomura, M. Shimamura, H. Tomizawa, and M. Usuda, Collapse of thin-walled curved beam with closed-hat section – Part 1: Study on collapse characteristics, *SAE Technical Paper* 1990; 900460.
- [16]. K. Hidekazu Nishigaki, S. Ishivama, M. Ohta, M. Takagi, F. Matsukawa, and M. Masanori, Collapse of thin-walled curved beam with closed-hat section – Part 2: Simulation by plane plastic hinge model, *SAE Technical Paper* 1990; 900461.
- [17]. C. Zhang and A. Saigal, Crash behavior of a 3D S-shape space frame structure. *Journal of Materials Processing Technology* 191, 2007, 256–9.
- [18]. P. Hosseini-Tehrani and M. Nikahd, Effects of ribs on S-frame crashworthiness. *Proceedings of the Institution of Mechanical Engineers Part D Journal of Automobile Engineering* 220, 2006,1679–89.
- [19]. P. Hosseini-Tehrani and M. Nikahd, Two materials S-frame representation for improving crashworthiness and lightening, *Thin-Walled Structures* 44, 2006,407–14.
- [20]. A. Reyes, M. Langseth, and O.S. Hopperstad, Crashworthiness of aluminum extrusions subjected to oblique loading: experiments and numerical analyses, *International Journal of Mechanical Sciences* 44, 2002, 1965–1984.
- [21]. T. Tran, S. Hou, X. Han, N.T. Nguyen, and M.Q. Chau, Theoretical prediction and crashworthiness optimization of multi-cell square tubes under oblique impact loading, *International Journal of Mechanical Sciences* 89, 2014, 177–193.
- [22]. A. Elmarakbi, Y.X. Long, and J. MacIntyre, Crash analysis and energy absorption characteristics of S-shaped longitudinal members, *Thin-Walled Structures* 68, 2013, 65–74.
- [23]. LS-DYNA, Livermore Software Technology Corporation. Livermore, California, USA; 2010.
- [24]. X. Zhang and H. Zhang, Energy absorption of multi-cells tube columns under axial compression, *Thin-Walled Structures* 68, 2013, 156–163.

- [25]. G. Sun, G. Li, S. Hou, S. Zhou, W. Li, and Li Q, Crash worthiness design for functionally graded foam-filled thin-walled structures, *Materials Science and Engineering: A* 527, 2010, 1911–1919.
- [26]. M.A. Guler, M.E. Cerit, B. Bayram, B. Gerceker, and E. Karakaya. The effect of geometrical parameters on the energy absorption characteristics of thin-walled structures under axial impact loading. *International Journal of Crashworthiness* 15, 2010, 377–390.
- [27]. E.K. Zavadskas, Z. Turskis, J. Tamošaitiene, and V. Marina, Multi criteria selection of project managers by applying grey criteria, *Technological and Economic Development* 14, 2008, 462–77.
- [28]. E.K. Zavadskas, A. Kaklauskas, Z. Turskis, and J. Tamošaitiene, Selection of the effective dwelling house walls by applying attributes values determined intervals, *Journal of Civil Engineering and Management* 14, 2008, 85–93.
- [29]. A. Kaklauskas, E.K. Zavadskas, and V. Trinkunas, A multiple criteria decision support on-line system for construction, *Engineering Applications of Artificial Intelligence* 20, 2007, 163–175.
- [30]. A. Kaklauskas, E.K. Zavadskas, S. Raslanas, R. Ginevicius, A. Komka, and P. Malinauskas, Selection of low-e windows in retrofit of public buildings by applying multiple criteria method COPRAS: A Lithuanian case. *Energy and Buildings* 38, 2006, 454–462.
- [31]. E.K. Zavadskas, A. Kaklauskas, F. Peldschus, and Z. Turskis, Multi-attribute assessment of road design solutions by using the COPRAS method, *Baltic Journal of Road and Bridge Engineering* 2, 2007, 195–203.
- [32]. N. Qiu, Y. Gao, J. Fang, Z. Feng, G. Sun, and Q. Li. Crashworthiness analysis and design of multi-cell hexagonal columns under multiple loading cases, *Finite Elements in Analysis and Design* 104, 2015, 89–101.
- [33]. G. Zheng, S. Wu, G. Sun, G. Li, and Q. Li, Crushing analysis of foam-filled single and bitubal polygonal thin-walled tubes, *International Journal of Mechanical Sciences* 87, 2014, 226–240.
- [34]. S. Wu, G. Zheng, G. Sun, Q. Liu, G. Li, and Q. Li, On design of multi-cell thin-wall structures for crashworthiness, *International Journal of Impact Engineering* 88, 2016, 102–117.
- [35]. C. Qi, S. Yang, and F. Dong, Crushing analysis and multiobjective crashworthiness optimization of tapered square tubes under oblique impact loading, *Thin-Walled Structures* 59, 2012, 103–119.
- [36]. A. Baroutaji, M.D. Gilchrist, D. Smyth, and A.G. Olabi, Crush analysis and multi-objective optimization design for circular tube under quasi-static lateral loading, *Thin-Walled Structures* 86, 2015, 121–131.
- [37]. A. Khalkhali, Best compromising crashworthiness design of automotive S-rail using TOPSIS and modified NSGAI, *Journal of Central South University* 22, 2015, 121–133.